An Unusual Natural Product Primary Sulfonamide: Synthesis, Carbonic Anhydrase Inhibition and Protein X-ray Structures of Psammaplin C

Prashant Mujumdar,[†] Kanae Teruya,[†] Kathryn F. Tonissen,[†] Daniela Vullo,[‡] Claudiu T. Supuran,[‡] Thomas S. Peat,[§] and Sally-Ann Poulsen[*,†]

[†]Eskitis Institute for Drug Discovery, Griffith University, Don Young Road, Nathan, Queensland 4111, Australia

[‡]Polo Scientifico, Neurofarba Department and Laboratorio di Chimica Bioinorganica, Universitàdegli Studi di Firenze, Via della Lastruccia 3, 50019 Sesto Fiorentino, Florence, Italy

[§]CSIRO, 343 Royal Parade, Parkville, Victoria 3052, Australia

[*]Corresponding author Tel: +61-7-37357825; E-mail: s.poulsen@griffith.edu.au

Abstract

Psammaplin C is one of only two described natural product primary sulfonamides. Here we report a new and alternate synthesis of psammaplin C and evaluate for the first time the inhibition profile of a natural product primary sulfonamide against therapeutically relevant carbonic anhydrase (CA) zinc metalloenzymes. The compound exhibited unprecedented inhibition of an important cancer-associated isozyme, hCA XII, with a K_i of 0.79 nM. The compound also displayed good isoform selectivity for hCA XII over other CAs. We present the first reported protein X-ray crystal structures of psammaplin C in complex with human CAs. We engineered the easily crystallized hCA II enzyme to mimic both the hCA IX and hCA XII binding sites and then utilized protein X-ray crystallography to determine the binding pose of psammaplin C within the hCA II, hCA IX and hCA XII mimic active sites, all to high resolution. This is the first time a natural product primary sulfonamide inhibitor has been assessed for inhibition and binding to CAs as well as structurally characterized bound to different CA proteins.

Introduction

Carbonic anhydrases (CA, EC 4.2.1.1) are zinc metalloenzymes that catalyze the reversible hydration of carbon dioxide to bicarbonate and a proton: $CO_2 + H_2O \leftrightarrows HCO_3^- + H^+$. This equilibrium is critical for human health, and blocking the endogenous chemistry catalyzed by CAs is a current target for therapeutic intervention.[1] Most reported small molecule CA inhibitors incorporate a primary sulfonamide functional group, this group blocks the enzymes activity by coordination to the catalytic zinc.[2] Natural products (NPs) offer extraordinary chemical diversity, and in recent times have been explored as a source of novel CA inhibitors. NPs so far identified that can inhibit CA are however not primary sulfonamides, instead they have an alternate zinc binding group (e.g. phenol or carboxylate group) within their structure.[3, 4] Given the prominence of the primary sulfonamide group in medicinal chemistry, we conducted a literature search of the *Dictionary of Natural Products* (DNP) database[5] and found just two primary sulfonamide NPs.[6] We recently reviewed the discovery, total synthesis, and known bioactivity for these compounds, which includes psammaplin C **1** (Figure 1).[6] This unusual NP was isolated in 1991 from the marine sponge *Pseudoceratina purpurea*.[7] The structure of **1** comprises a bromotyrosine-oxime functionalized scaffold. Compound **1** was assessed for histone deacetylase (HDAC) inhibition activity and had no activity against this metalloenzyme[8], which has a preference for hydroxymate as the zinc binding group.[9] Compound **1** has not before been investigated for interaction with CA enzymes. Our aim was to synthesize NP **1** and evaluate the bioactivity against a comprehensive panel of human CA (hCA) isozymes. We were also interested to assess the binding pose of this unusual NP within the hCA active sites and determine the protein X-ray structure of **1** in complex with hCA II and recently generated mimics of hCA IX and hCA XII.

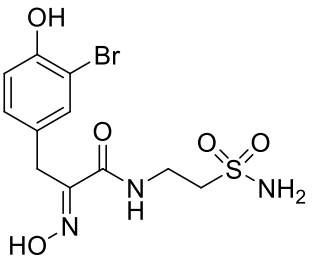

1

Figure 1. Psammaplin C **1** − an unusual natural product comprising a primary sulfonamide group.

Results and Discussion

Chemical Synthesis. We encountered two difficulties with the reported synthetic route of NP **1**. Firstly, the synthesis employs a bis-*O*-benzyl protected oxime acid as the key intermediate,[10] however the conditions described to generate this intermediate were ambiguous, and our efforts to optimize this step were not successful. Another drawback of the known synthetic method was the need for the strong Lewis acid, TMSI for *O*-benzyl ether deprotection in the final step towards **1**. TMSI is extremely moisture sensitive and inconvenient to handle. We sought to develop an alternate synthesis of **1** in order to circumvent the limitations encountered with the reported synthetic route.

Our synthesis is an adaptation of the synthesis reported for the related disulfide metabolite psammaplin A, Scheme 1.[11, 12] Reaction of commercially available 3-bromo-4-hydroxy benzaldehyde **2** with *N*-acetyl glycine under Erlenmeyer conditions generated the benzylidene oxazolone **3**. Compound **3** was converted to the α-keto acid **4** (enol form) by acid hydrolysis. Subsequent oximation of **4** with THP hydroxylamine gave the mono *O*-THP protected oxime acid **5**. Treatment of **5** with *N*- hydroxysuccinimide and EDC afforded an activated succinate ester derivative, which after work up, was immediately reacted with β-aminoethanesulfonamide hydrochloride **11** to generate the *O*-THP protected psammaplin C

derivative **6**. Finally, the THP group of **6** was removed using 4M HCl in dioxane[13] to furnish the target NP **1** in as white solid. The key advantage of this new synthetic route rests with the implementation of the THP protecting group in lieu of the benzyl protecting groups of the earlier reported synthesis. Introduction of the *O*-THP protected oxime acid, compound **9**, was straightforward and required mild reaction conditions (4M HCl in dioxane) to deprotect the oxime-THP group. Significantly, only the oxime oxygen requires protection, while the phenol hydroxyl group does not, a further advantage of this alternative synthetic route. We anticipate that the mild conditions and good yields associated with this synthesis will facilitate ready access to further primary sulfonamide analogues of **1**.

Scheme 1. Synthesis of NP **1**.

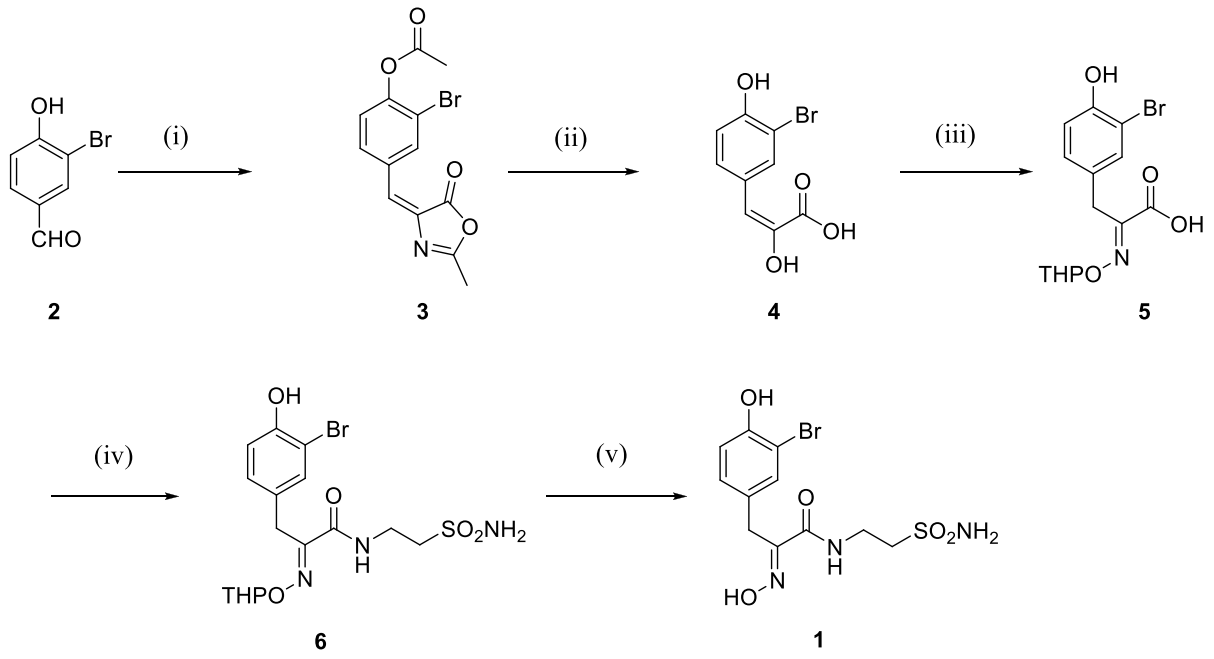

Reagents and Conditions: (i) *N*-acetyl glycine, NaOAc, Ac_2O, 120 °C, 3 h, 85%; (ii) Aq. HCl (10%), reflux, 15 h, 65%; (iii) H_2NOTHP, dry pyridine, rt, 15 h, 54%; (iv) a) EDC.HCl, HOSu, dry 1,4-dioxane, 2-3 h, rt; b) beta-aminoethanesulfonamide hydrochloride **11**, dry NEt_3, dry MeOH, rt, 12 h, 46% (over 2 steps); (v) 4.0 M HCl in 1,4-dioxane, 0 °C, 6-8 h, 80%.

The required coupling agent β−aminoethanesulfonamide hydrochloride **11** was prepared using a combination of previous methods (Scheme 2).[14, 15] The amino functionality of taurine **7** was first protected with phthalimide to provide the sodium salt **8**, which was subsequently chlorinated using PCl_5 to furnish the sulfonyl chloride **9**. Compound **9** was treated with aq. NH_4OH to provide primary sulfonamide **10**. Finally, deprotection of the phthalimido group of **10** was carried out using hydrazine hydrate to generate β−aminoethanesulfonamide **11** as the hydrochloride salt.

Scheme 2. Synthetic route to β−aminoethanesulfonamide hydrochloride **11**.

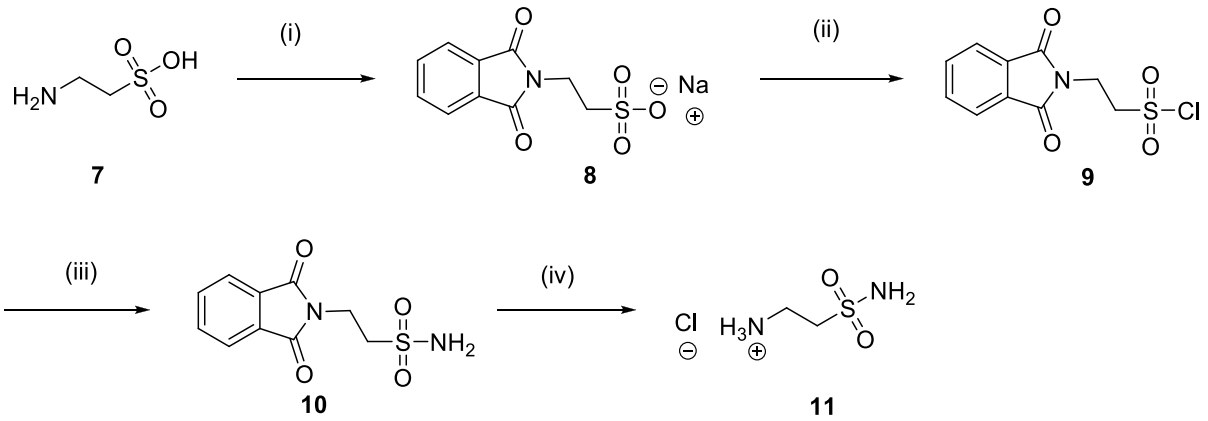

Reagents and Conditions: (i) Phthalic anhydride, Na_2CO_3, AcOH, reflux, 5 h, 89%; (ii) PCl_5, dry toluene, reflux, 5 h, 92%; (iii) Aq. NH_4OH (30%) + 1,4-dioxane (1:1), ACN, 0 °C-rt, 4 h, 54%; (iv) NH_2NH_2 .xH_2O (55%), EtOH, conc. HCl, reflux, 3 h, 51%.

The oxime geometry of precursor **6** and the target NP **1** was confirmed as *E* on the basis of ^{13}C NMR data reported for the structurally related disulfide metabolites **12** (*E*) and **13** (*Z*) (Figure 2).[16] The benzylic carbon of **12** resonates at δ26.7, and is upfield of the corresponding carbon in **13** (δ35.7). This chemical shift difference is consistent with an *E* to *Z* oxime configuration change.[17]

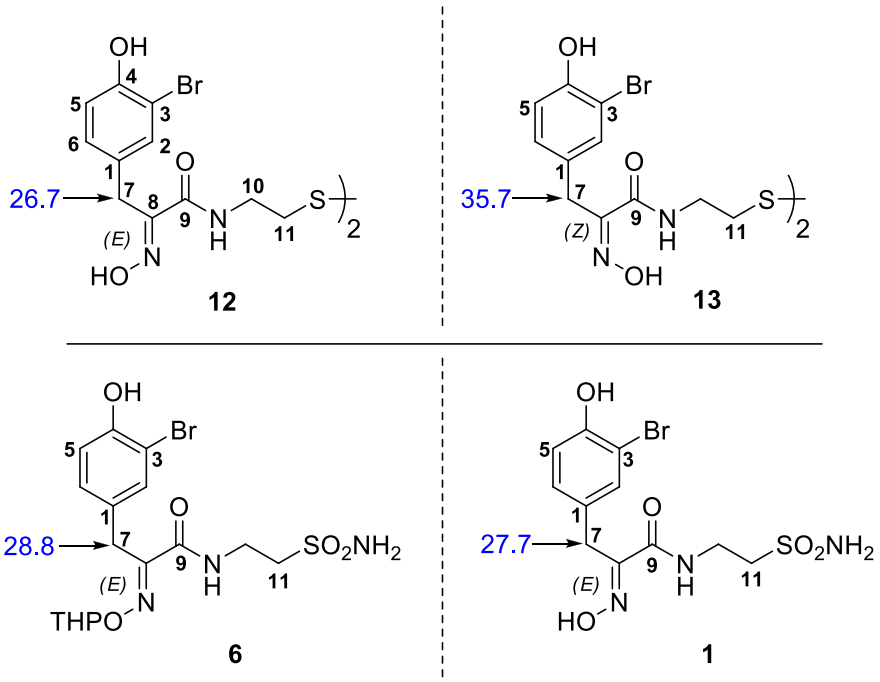

Figure 2. ^{13}C NMR chemical shifts (blue) of precursor **6** and the target NP **1** and known compounds **12** and **13** are consistent with the *E* configuration of the oxime moiety.

CA Inhibition. The CA inhibition data for **1** and reference compound acetazolamide (**AZA**), the *par excellence* therapeutically established CA inhibitor, was measured against a panel of hCA isozymes (Table 1). Compared to **AZA**, the NP **1** showed remarkable variation among the different CA isoforms, with a range of inhibition constants (K_i's) that span five orders of magnitude (K_i range 0.79 nM – 10630 nM), while for **AZA** the CA inhibition is more tightly grouped (K_i range 2.5 – 250 nM). Compound **1** had exceptional inhibition for hCA XII, with a K_i of 0.79 nM (entry 8, Table 1). Although low nanomolar CA inhibitors are widely known, subnanomolar CA inhibition is uncommon. hCA XII expression is upregulated in a wide selection of hypoxic tumors and has recently been identified as a key player in the facilitation of P-glycoprotein mediated multidrug resistance in cancer cell models.[18] Compound **1** may thus provide a valuable probe compound for biology associated with CAs, and with hCA XII

in particular. Compound **1** has been submitted to the Compounds Australia Open Compound Collection (Academic) (https://www.griffith.edu.au/science-aviation/compounds-australia).[19]

Table 1. Human CA inhibition profile for NP **1** and the reference CA inhibitor **AZA**.

Entry	**hCA isoform**	K_i **(nM)**[#]	
		1	**AZA**
1	hCA I	48.1	250
2	hCA II	88.0	12
3	hCA IV	75.3	74.2
4	hCA VA	154	63.1
5	hCA VI	9680	11.0
6	hCA VII	1.7	2.5
7	hCA IX	12.3	25.0
8	hCA XII	0.79	5.7
9	hCA XIII	10630	16.4
10	hCA XIV	379	41.3

#Errors ± 10% of the reported values (from three separate assays).

Protein X-Ray Crystal Structures. Atomic level structures with the novel NP **1** bound to different CA isozymes would allow us to look at the differences in interactions between **1** and the different active sites in detail. **AZA** is very compact in size relative to **1**, and so is not able to directly interact with the variable outer rim hCA active site residues. We engineered the hCA II protein to mimic the active sites of hCA IX and hCA XII. This approach has been used a number of times to facilitate the structural biology of proteins recalcitrant to crystallization, including CA IX,[20] this is however the first CA XII mimic.

The protein sequences for hCA IX and hCA XII were aligned to the hCA II sequence, highlighting 14 conserved residues between the three sequences found in the active site, these were retained in the mimic proteins: N62, H64, Q92, E106, V121, L141, V143, L198, T199, T200, P201, P202, V207 and W209, Figure 3. The three dimensional structure of hCA II was analyzed manually with the sequences of hCA IX and hCA XII superposed on all of the active site residues. Ten substitutions were made to the hCA II sequence to obtain the hCA IX mimic protein: A65S, N67Q, E69T, I91L, F131V, G132D, V135L, K170E, L204A and C206G; while nine substitutions were made to obtain the hCA XII mimic protein: A65S, N67K, E69N, I91T, F131A, G132S, V135S, L204N and C206T, Figure 3.

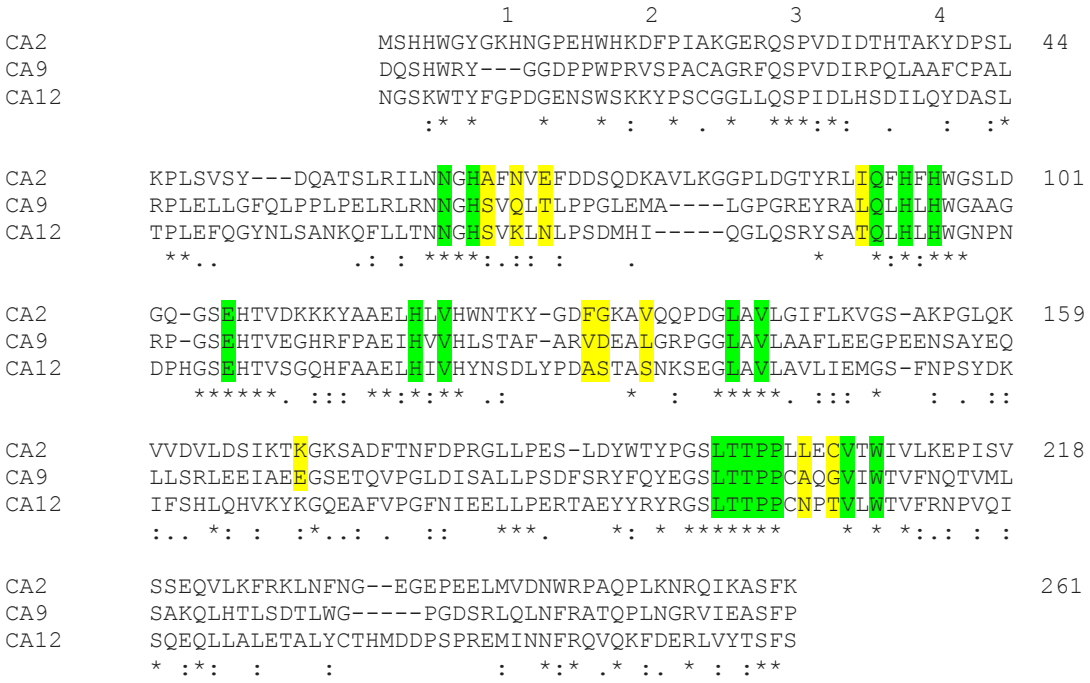

Figure 3. Amino acid sequence alignment of the catalytic domain of hCA II, IX and XII. Conserved residues are highlighted in green, while CA II residues highlighted in yellow were replaced with the corresponding CA IX and CA XII residues, to create the mimic proteins.

Capasso and co-workers recently reported a rapid and facile in-gel technique to enable determination of CA activity and the corresponding molecular weight.[21] The utility of this technique, known as protonography, as a CA activity assay has since been reported for multiple classes of CAs including bovine CA (α-CA), recombinant CA from *Vibrio cholerae* (VchCA, α-CA),[21] *Porphyromonas gingivalis* (PgiCA, γ-CA),[22] and *Plasmodium falciparum* (PfCA, η-CA),[23] and native CAs in whole cell lysate of *Escherichia coli* (β- and γ-CAs).[21] In this technique, an SDS gel loaded with CAs is stained with bromothymol blue, a commonly used pH indicator for pH range between 6.0 and 7.6. The stained gel is then suspended in carbonated water. An immediate color change from blue to yellow is observed at the position of catalytically active CA as a result of local acidification (due to H^+ ions generated by CA hydratase activity). Here we have applied protonography to assess the activity of hCA IX and hCA XII. Both mimic proteins generated a strong yellow band, consistent with the mimics retaining the enzymatic activity of the parent hCA II (Figure 4, lanes 1-3). Control proteins (bovine serum albumin, BSA, and ovalbumin, OVA) did not generate a color change, confirming the color change observed is dependent on CA activity (Figure 4, lane 4-6).

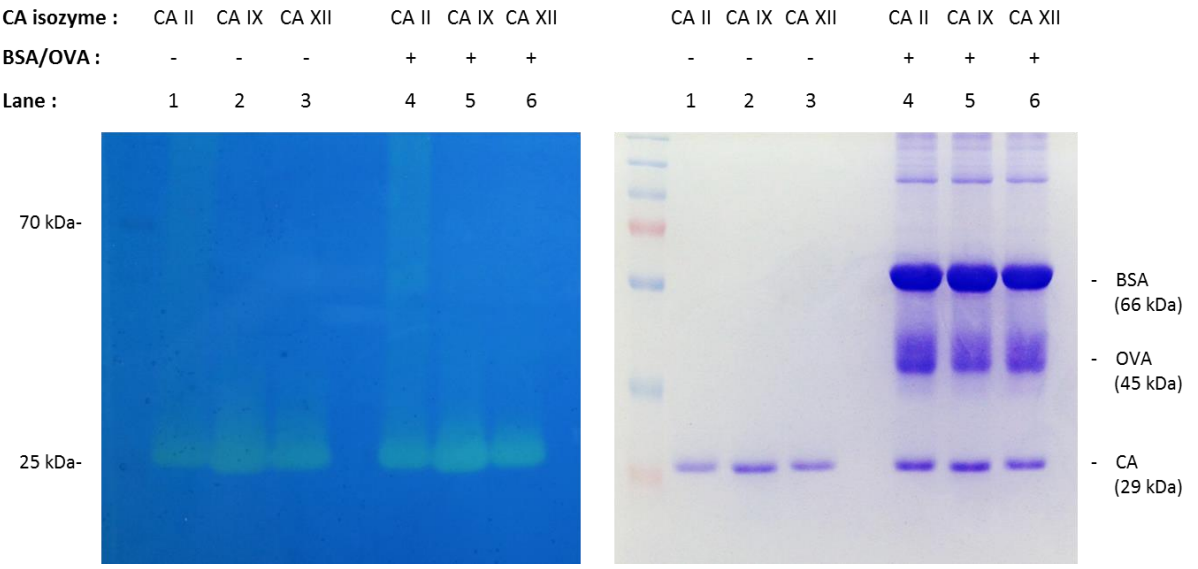

Figure 4. Protonogram (left) and coomassie blue stain (right) of recombinant hCA II, CA IX mimic, and CA XII mimic (0.5 μg each). The yellow signal at approximately 29 kDa confirms CA enzymatic activity (lane 1-3), which was not observed for non-CA proteins (lane 4-6).

X-ray crystal structures of the apo forms of the hCA IX and hCA XII mimic proteins were determined to look at the potential differences between the native active sites. There are no substantial changes (beyond a few sidechain rotamers) that occur between the apo and compound **1**-bound structures of the CA IX and XII mimic proteins, so we focus on the bound structures. A comparison of the CA XII mimic structure to a previously elucidated crystal structure of human CA XII (Figure 5, PDB code 4HT2)[24] shows that the active sites are very similar, differing only at the rim of the active site where there is a small change in the position of a loop-helix (residues 127-139 (124-137 in 4HT2), an average of ~2 Å in Cα positions, with a 2.4 Å maximum difference). Overall the CA XII mimic when compared with PDB entry 4HT2, shows some regional backbone variations remote from the active site, with the overall rmsd between the mimic and 4HT2 of 1.24 Å to 1.18 Å (A and B chains, respectively), with 11 gaps over 242 aligned residues (of 258), with 41% sequence identity. Figure 6 shows the X-ray crystal structures of hCA II and the hCA IX and hCA XII mimics in complex with compound **1**. These data for the [hCA II:**1**] complex extend to 1.57 Å resolution, for the [hCA IX:**1**] complex to 1.35 Å resolution and for the [hCA XII:**1**] complex to 1.40 Å resolution (see supporting information, Table 1).

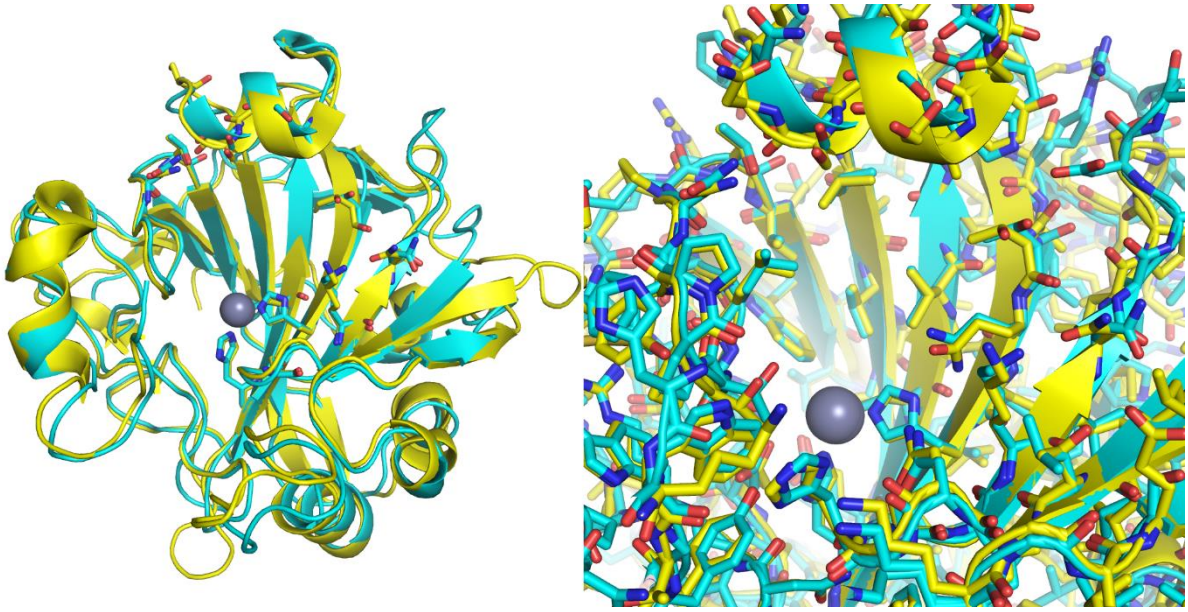

Figure 5. A comparison of the CA XII mimic with the previously determined CA XII structure 4HT2 in the PDB. The CA XII mimic is in cyan with 4HT2 in yellow; the grey sphere represents the zinc atom in the active site. The left panel highlights the mutations made in the active site of CA II to make the CA XII mimic. The most significant difference is found at the top (12 o'clock) at the rim of the active site, where a small helix is translated about 2 Å.

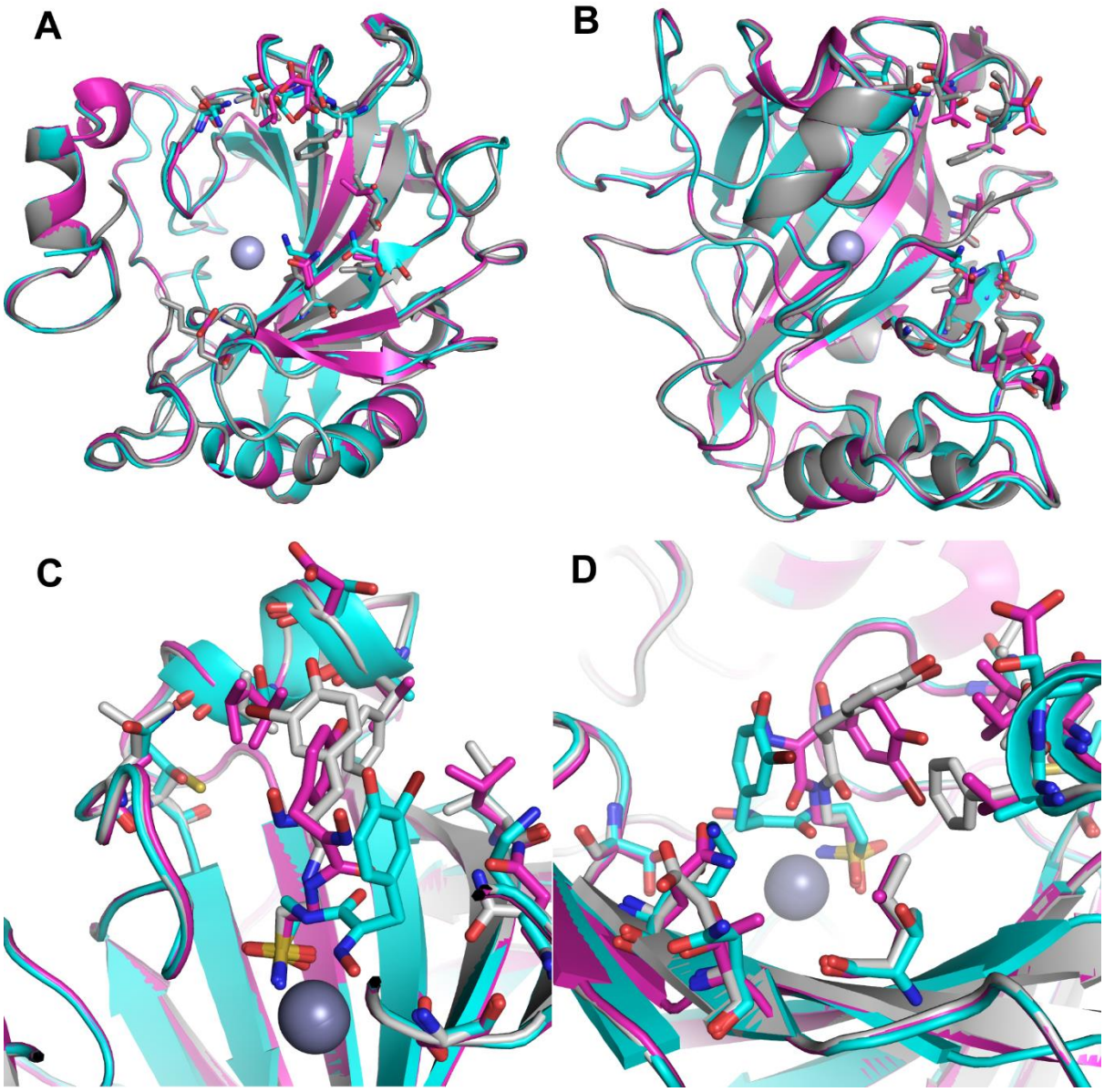

Figure 6. The X-ray crystal structures of hCA II and the hCA IX and hCA XII mimics. Panels A and B highlight the sequence changes made to create the mimic proteins; CA II is in grey, CA IX in magenta and CA XII in cyan; the two orientations in A and B are approximately a 90 degree rotation from each other. Panels C and D show compound **1** as bound to the three different proteins; C and D are approximately 90 degrees rotated from each other. The grey sphere represents the zinc atom in the active site of the proteins. It is clear that compound **1** adopts a different orientation in each of the three structures, although the sulfonamide moiety is in almost the same position for each structure.

Except in the [hCA IX:**1**] complex, where little of the extended structure of compound **1** beyond the sulfonamide is seen, compound **1** makes multiple interactions with the protein as it extends out of the catalytic pocket (see supporting information). There was clear density for the sulfonamide moiety of compound **1** adjacent to the zinc atom in the active sites after the initial rounds of refinement for all of the complexes. The sulfonamide functional group interacts directly with the zinc and has potential hydrogen bonds to active site residue Thr199 with the same pose as that for >200 sulfonamide/hCA II complexes reported in the PDB. In the [hCA II:**1**] complex, the amide nitrogen is 2.95 Å from the Thr200 side chain and the amide oxygen is bound to a water molecule, which is close to Gln92. The nitrogen of the oxime is within hydrogen bonding distance to the Thr200 side chain and the hydroxyl of the oxime is 2.6 Å to the Pro201 carbonyl. In the [hCA XII:**1**] complex, the nitrogen of **1** in the amide linker is 3.1 Å from the Thr200 side chain and the amide oxygen is directly bound (2.7 Å) to the side chain of Gln92. In this complex, the oxime oxygen is bound to a water molecule at 2.7 Å; this water molecule is also coordinated by hydrogen bonds to Tyr7 and His64. In both complexes, compound **1** is not modelled at full occupancy (about 80%) and there is some additional positive electron density in the difference maps, suggesting that there are other conformations of **1** that may be possible in the active site.

The bromophenol moiety sits in a hydrophobic pocket made up of Phe131, Val135, Pro202 and Leu204 at 3.7 to 4.7 Å with no obvious hydrogen bonds in the [hCA II:**1**] complex. This is reminiscent of the interactions made by the hydrophobic tail of brinzolamide in hCA II as reported by Pinard et al,[20] but the bromine atom is buried even tighter into this pocket than the hydrophobic tail of brinzolamide. The ring of the bromophenol moiety of the [hCA XII:**1**] complex has close contacts with the Asn62 side chain at 3.1 Å. The bromine's closest contact to the hCA XII mimic is 4 Å to the Lys67 side chain, but it makes closer contacts to a second

molecule of **1** found at the top of the active site (about 3.7 Å away). There is also a second molecule of **1** in the [hCA II:**1**] complex found nearby which has the bromophenol moiety bound between the His3 ring and the bromophenol ring of **1** bound to the zinc. This second molecule of **1** has the hydroxyl moiety making a potential hydrogen bond to the Trp5 ring nitrogen, with the rest of the compound solvent exposed. In the [hCA II:**1**] complex there is even a third molecule of **1** found in the structure completely outside the active site and between crystallographically related monomers (see supporting information). All of the complex models refined well against the data (see Table 1 of the supplementary information).

Conclusion

In conclusion, psammaplin C (**1**) occupies a rare place in NP chemical space, as one of only two primary sulfonamide NPs so far isolated and characterized. Herein we have developed an improved and facile synthesis of **1** and confirmed the *E* stereochemistry about the oxime center. We have evaluated for the first time the CA inhibition characteristics for this unusual NP against a panel of ten human CA isoforms. Notably, the NP exhibited a distinctive CA inhibition profile when compared to the somewhat flat inhibition profile of **AZA**. Compound **1** is a subnanomolar inhibitor of an important cancer-associated isozyme, hCA XII, and displayed good isoform selectivity for hCA XII. We engineered the easily crystallized hCA II enzyme to mimic both the hCA IX and hCA XII binding sites, both exhibited catalytic activity. We utilized protein X-ray crystallography to determine the binding pose of **1** within the hCA II, hCA IX and hCA XII mimic active sites, all to high resolution. The NP engages in a series of strong interactions with the active site residues of hCA II and hCA XII and represents the first reported structures of a NP sulfonamide with hCA enzymes.

Experimental Section

General Chemistry. All reactions were carried out in dry solvents under anhydrous conditions, unless otherwise mentioned. All chemicals were purchased commercially and used without further purification. All reactions were monitored by TLC using silica plates with visualization of product bands by UV fluorescence (λ = 254 nm) and charring with Vanillin (6 g vanillin in 100 mL of EtOH containing 1% (v/v) concentrated sulfuric acid) stain. Silica gel flash chromatography was performed using silica gel 60 Å (230-400 mesh). NMR (^{1}H, ^{13}C, COSY, HSQC and HMBC) spectra were recorded on the 500 MHz spectrometer at 25°C. Chemical shifts for ^{1}H and ^{13}C NMR obtained in DMSO-d_6 are reported in ppm relative to residual solvent proton (δ = 2.50 ppm) and carbon (δ = 39.5 ppm) signals respectively. Multiplicity is indicated as follows: s (singlet); d (doublet); t (triplet); q (quartet); m (multiplet); dd (doublet of doublet); bs (broad signal). Coupling constants are reported in hertz (Hz). High- and low-resolution mass spectra were acquired using electrospray as the ionization technique in positive-ion and/or negative-ion modes as stated. All MS analysis samples were prepared as solutions in methanol. Purity of compounds (**1** and **6**) was determined by HPLC instrument (Agilent 1100 series) with UV detection. The melting points are uncorrected. Numbering used for NMR assignments is shown below.

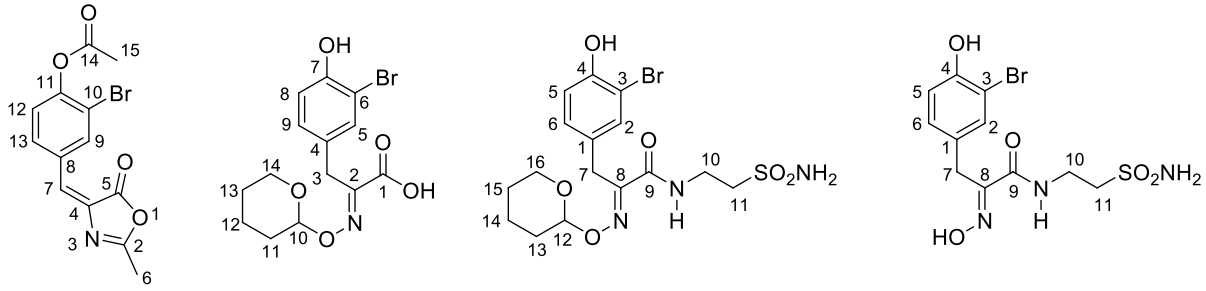

2-Bromo-4-{[(4*E*)-2-methyl-5-oxo-4,5-dihydro-1,3-oxazol-4-ylidene]methyl}phenyl acetate (3)

To a mixture of anhydrous NaOAc (1.47 g, 17.90 mmol, 1.2 equiv) and *N*-acetyl glycine (2.01 g, 17.90 mmol, 1.2 equiv) suspended in Ac_2O (15.23 g, 149.2 mmol, 10 equiv) at room

temperature under inert atmosphere, was added 3-bromo-4-hydroxybenzaldehyde **2** (3.0 g, 14.92 mmol, 1 equiv). The resulting mixture was stirred at 120 °C for 4 h and then cooled to room temperature. After complete precipitation, the solid was poured into ice cold water (25-30 mL) and vigorously stirred for 15 min. The mixture was then filtered and residual solid dried under vacuum to obtain title compound **3** (4.11 g, 85.3%, crude) as yellow solid. The crude product was used for the next step without further purification. A minimal amount of crude product was purified by flash chromatography (5-8% acetone in *n*-hexane) for characterization purposes. R_f = 0.46 (20% acetone in *n*-hexane). Mp = 196−198°C. ^{1}H NMR (500 MHz, DMSO-d_6) δ_H = 8.55 (s, 1H, H-9); 8.22 (d, J = 8.5 Hz, 1H, H_{Ar}); 7.44 (d, J = 8.5 Hz, 1H, H_{Ar}); 7.24 (s, 1H, H-7); 2.41 (s, 3H, H-6); 2.35 (s, 3H, H-15), general assignments were confirmed by ^{1}H-^{1}H gCOSY. ^{13}C NMR (125 MHz, DMSO-d_6) δ_C = 168.0 (C_{quat}); 167.6 (C_{quat}); 166.9 (C_{quat}); 149.3 (C_{quat}); 135.7 (C-9); 133.6 (C_{quat}); 132.8 (C_{quat}); 132.3 (CH_{Ar}); 126.9 (C-7); 124.6 (CH_{Ar}); 116.1 (C_{quat}); 20.5 (C-15); 15.4 (C-6), general assignments were confirmed by ^{1}H-^{13}C HSQC. LRMS (ESI$^+$): m/z = 324, 326 [M+H; ^{79}Br, ^{81}Br]$^+$.

(2*E*)-3-(3-Bromo-4-hydroxyphenyl)-2-hydroxyprop-2-enoic acid (4)

To the crude oxazolone **3** (3.0 g, 9.29 mmol, 1.0 equiv) was added 10% aq. HCl (93 mL, 10 mL/mmol) and the resulting reaction mixture stirred at reflux (102-104°C) for 12-14 h. The reaction mixture was cooled to room temperature and the product extracted in EtOAc (3 × 25 mL). The combined organic fractions were washed with saturated aqueous NaCl (1 × 20 mL/mmol), dried over $MgSO_4$ and concentrated *in vacuo* to provide crude aryl pyruvic acid **4** (1.57 g, 65.55%, crude) as a light brown solid. The crude aryl pyruvic acid was used for the next step without further purification. ^{1}H NMR (500 MHz, DMSO-d_6) δ_H = 10.40 (s, 1H); 9.11 (s, 1H); 8.02 (d, J = 1.9 Hz, 1H); 7.50 (dd, J = 8.5, 1.9 Hz, 1H); 6.93 (d, J = 8.45 Hz, 1H); 6.31

(s, 1H). ^{13}C NMR (125 MHz, DMSO-*d*$_6$) δ_C = 166.3, 153.3, 140.4, 133.3, 130.1, 127.8, 116.1, 109.3, 108.7; LRMS (ESI$^-$): *m/z* = 257, 259 [M−H; ^{79}Br, ^{81}Br]$^+$.

(2*E*)-3-(3-Bromo-4-hydroxyphenyl)-2-[(oxan-2-yloxy)imino]propanoic acid (5)

To a mixture of the arylpyruvic acid **4** (1.5 g, 5.81 mmol, 1.0 equiv) and *O*-(tetrahydro-*2H*-pyran-2-yl) hydroxylamine (1.02 g, 8.71 mmol, 1.5 equiv) was added anhydrous pyridine (11.6 mL, 2 mL/mmol) under an argon atmosphere. The resulting reaction mixture was stirred overnight (12-14 h) at room temperature. Pyridine was removed *in vacuo*, to the residue was added 1N HCl (32 mL, 5.5 mL/mmol) and extracted in EtOAc (3 × 25 mL). The combined organic fractions were washed with saturated aqueous NaCl (1 × 20 mL/mmol), dried over $MgSO_4$ and concentrated *in vacuo*. Column chromatography of the crude residue afforded the title compound **5** (1.12 g, 54.0%) as a pale yellow solid. R_f = 0.11 (10% MeOH in DCM). Mp = 42−44°C. ^{1}H NMR (500 MHz, DMSO-*d*$_6$) δ_H = 13.26 (bs, 1H, -COOH), 10.11 (s, 1H, Ar-OH), 7.36-7.35 (d, *J* = 2.1 Hz, 1H, H-5); 7.03 (dd, *J* = 8.35, 2.1 Hz, 1H, H-9); 6.88 (d, *J* = 8.3 Hz, 1H, H-8); 5.36-5.35 (m, 1H, H-10); 3.77 (d, *J* = 13.5 Hz, 1H, C*H*$_3$H); 3.73 (d, *J* = 13.5 Hz, 1H, CH*H*$_3$); 3.50-3.48 (m, 2H, H_{THP}); 1.76-1.71 (m, 3H, H_{THP}); 1.61-1.52 (m, 2H, H_{THP}); 1.48-1.45 (m, 1H, H_{THP}), general assignments were confirmed by ^{1}H-^{1}H gCOSY. ^{13}C NMR (125 MHz, DMSO-*d*$_6$) δ_C = 164.5 (C-1), 152.6 (C_{Ar}), 151.8 (C-2), 133.1 (C-5), 129.0 (C-9), 128.1 (C_{Ar}), 116.3 (C-8), 109.0 (C_{Ar}), 100.8 (C-10), 61.2 (CH_2-THP), 29.7 (C-3), 28.1 (CH_2-THP), 24.6 (CH_2-THP), 18.4 (CH_2-THP), general assignments were confirmed by ^{1}H-^{13}C HSQC. LRMS (ESI$^+$): *m/z* = 380, 382 [M+Na; ^{79}Br, ^{81}Br]$^+$.

(2*E*)-3-(3-Bromo-4-hydroxyphenyl)-2-[(oxan-2-yloxy)imino]-N-(2-sulfamoylethyl)propanamide (6)

To a mixture of *O*-THP protected oximino acid **5** (0.29 g, 0.81 mmol, 1.0 equiv), EDC.HCl (0.26 g, 1.38 mmol, 1.7 equiv) and HOSu (0.18 g, 1.54 mmol, 1.9 equiv) under Ar atmosphere was added anhydrous 1,4-dioxane (8 mL, 10 mL/mmol) and the resulting solution was stirred at room temperature for 3 h. The solvent was evaporated under vacuum and the residue was dissolved in EtOAc (30-35 mL), washed with saturated aqueous $NaHCO_3$ (2 × 15 mL/mmol), 1N aqueous HCl (2 × 15 mL/mmol) and saturated aqueous NaCl (1 × 20 mL/mmol). The organic fraction was dried over $MgSO_4$ and concentrated *in vacuo* to afford crude succinate ester (0.37 g, 0.81 mmol, 1.0 equiv). The succinate ester was dissolved in anhydrous 1,4-dioxane (8 mL, 10 mL/mmol) under Ar atmosphere and a solution of β-aminoethanesulfonamide hydrochloride **11** (0.15 g, 0.93 mmol, 1.15 equiv) and NEt_3 (0.15 mL, 1.07 mmol, 1.15 equiv of **11**) in anhydrous MeOH (5 mL/mmol) was added. The resulting reaction mixture was stirred at room temperature for overnight (12-14 h). The solvent was then evaporated *in vacuo* to obtain the crude residue. Column chromatography (gradient 2.5−4% MeOH in DCM) of this crude residue gave title compound **6** (0.173 g, 46.75% over two steps) as a white solid. R_f = 0.21 (10% MeOH in DCM). Mp = 68−70°C. ^{1}H NMR (500 MHz, DMSO-d_6) δ_H = 10.08 (s, 1H, Ar-OH); 8.29 (t, *J* = 5.85 Hz, 1H, N-H); 7.38 (d, *J* = 2.05 Hz, 1H, H-2); 7.04 (dd, *J* = 8.3, 2.1 Hz, 1H, H-6); 6.93 (s, 2H, SO_2NH_2); 6.86 (d, *J* = 8.25 Hz, 1H, H-5); 5.35-5.34 (m, 1H, H-10); 3.77 (d, *J* = 13.15 Hz, 1H, CH_7H); 3.70 (d, *J* = 13.15 Hz, 1H, CHH_7); 3.60-3.51 (m, 2H, H-10); 3.47-3.45 (m, 2H, H_{THP}); 3.16 (t, *J* = 7.25 Hz, 2H, H-11); 1.75-1.73 (m, 3H, H_{THP}); 1.63-1.54 (m, 2H, H_{THP}); 1.48-1.45 (m, 1H, H_{THP}), general assignments were confirmed by ^{1}H-^{1}H gCOSY. ^{13}C NMR (125 MHz, DMSO-d_6) δ_C = 162.4 (C-9), 153.0 (C_{Ar}), 152.5 (C-8), 133.3 (C-2), 129.1 (C-6), 128.2 (C_{Ar}), 116.2 (C-5), 108.9 (C_{Ar}), 100.6 (CH-THP), 61.1 (CH_2-THP), 53.3 (C-11), 34.4 (C-10), 28.8 (C-7), 28.2 (CH_2-THP), 24.6 (CH_2-THP), 18.3 (CH_2-THP), general assignments were confirmed by ^{1}H-^{13}C HSQC. LRMS (ESI^+): *m/z* = 464, 466 [M+H; ^{79}Br, ^{81}Br]$^+$, 486, 488 [M+Na; ^{79}Br, ^{81}Br]$^+$. HRMS (ESI): calcd for

$C_{16}H_{22}BrN_3NaO_6S$ [M+Na; ^{79}Br] 486.0305, found 486.0296; calcd $C_{16}H_{22}BrN_3NaO_6S$ [M+Na; ^{81}Br] 488.0291, found 488.0275

(2*E*)-3-(3-Bromo-4-hydroxyphenyl)-2-(N-hydroxyimino)-N-(2-sulfamoylethyl)propanamide (1)

To the oxime THP ether **6** (0.125 g, 0.27 mmol, 1.0 equiv) was added 4M HCl in 1,4-dioxane solution (4.1 mL, 15 mL/mmol) at 0 °C, the reaction mixture was stirred at the same temperature. After completion of reaction (6−8 h, TLC), the solvent was evaporated *in vacuo* to obtain the crude residue. Column chromatography (gradient 4−6% MeOH in DCM) of this crude residue gave title compound **1** (0.082 g, 80.39%) as a white solid. R_f = 0.11 (10% MeOH in DCM). Mp = 160−162°C. ^{1}H NMR (500 MHz, DMSO-d_6) δ_H = 11.93 (s, 1H, N-OH); 10.03 (s, 1H, Ar-OH); 8.08 (t, *J* = 5.95 Hz, 1H, N-H); 7.29 (d, *J* = 2.1 Hz, 1H, H-2); 7.01 (dd, *J* = 8.35, 2.1 Hz, 1H, H-6); 6.93 (s, 2H, SO_2NH_2); 6.84 (d, *J* = 8.3 Hz, 1H, H-5); 3.68 (s, 2H, H-7); 3.54 (q, *J* = 6.35 Hz, 2H, H-10); 3.14 (t, *J* = 6.65 Hz, 2H, H-11), general assignments were confirmed by ^{1}H-^{1}H gCOSY. ^{13}C NMR (125 MHz, DMSO-d_6) δ_C = 163.1 (C-9), 152.3 (C_{Ar}), 151.5 (C-8), 132.8 (C-2), 129.1 (C-6), 128.8 (C_{Ar}), 116.1 (C-5), 108.8 (C_{Ar}), 53.5 (C-11), 34.1 (C-10), 27.7 (C-7), general assignments were confirmed by ^{1}H-^{13}C HSQC and HMBC. LRMS (ESI$^+$): *m/z* = 379, 381 [M+H; ^{79}Br, ^{81}Br]$^+$, 401, 403 [M+Na; ^{79}Br, ^{81}Br]$^+$. HRMS (ESI): calcd for $C_{11}H_{14}BrN_3NaO_5S$ [M+Na; ^{79}Br] 401.9730, found 401.9734; calcd for $C_{11}H_{14}BrN_3NaO_5S$ [M+Na; ^{81}Br] 403.9709, found 403.9711

Sodium 2-(1,3-dioxo-2,3-dihydro-1H-isoindol-2-yl)ethane-1-sulfonate (8)

Taurine **7** (3.0 g, 23.97 mmol), anhydrous sodium acetate (2.08 g, 25.40 mmol, 1.06 equiv) suspended in glacial AcOH (30 mL, 1.25 mL/mmol) was stirred at reflux temperature for 30 min followed by addition of phthalic anhydride (3.76 g, 25.40 mmol, 1.06 equiv). The resulting

mixture was refluxed for next 4 hours. The reaction mixture was cooled at room temperature then in ice bath and filtered. The solid was washed with AcOH (20 mL) and MeOH (20 mL) to afford the title compound as white solid (5.95 g, 89%). ^{1}H NMR (500 MHz, D_2O) δ_H = 7.89-7.87 (m, 4H); 4.11 (t, *J* = 6.7 Hz, 2H); 3.32 (t, *J* = 6.65 Hz, 2H); ^{13}C NMR (125 MHz, D_2O) δ_C = 169.9, 134.8 (2 carbons), 131.2, 123.4 (2 carbons), 47.8, 33.4; LRMS (ESI^+): *m/z* = 278 $[M+H]^+$.

2-(1,3-Dioxo-2,3-dihydro-1H-isoindol-2-yl)ethane-1-sulfonyl chloride (9)

Sodium-3-phthalimidopropane-1-sulfonate **8** (5.5 g, 19.84 mmol, 1.0 equiv) suspended in dry toluene (40 ml, 2.05 ml/mmol) was stirred at reflux temperature under Ar atmosphere. To this hot mixture was added PCl_5 (4.13 g, 19.84 mmol, 1.0 equiv) in portions and the reaction mixture was stirred at reflux temperature for 1.5 h. A second portion of PCl_5 (4.13 g, 19.84 mmol, 1.0 equiv) was added in portions and the reaction mixture was refluxed for next 1.5 h. The reaction mixture was evaporated in vacuo, to the residual solid was added ice and allowed to stand for 20-30 min. The solid filtered and dried in vacuo to afford the title compound as white solid (5.04 g, 92%). R_f = 0.33 (30% EtOAc in n-hexane). Mp = 161−163 °C. ^{1}H NMR (500 MHz, $CDCl_3$) δ_H = 7.90-7.87 (m, 2H); 7.78-7.74 (m, 2H); 4.36 (t, *J* = 6.55 Hz, 2H); 4.09 (t, *J* = 6.55 Hz, 2H); ^{13}C NMR (125 MHz, $CDCl_3$) δ_C = 167.5, 134.7 (2 carbons), 131.8, 123.9 (2 carbons), 61.5, 32.9; LRMS (ESI^+): *m/z* = 274 $[M+H]^+$, 296 $[M+Na]^+$.

2-(1,3-Dioxo-2,3-dihydro-1H-isoindol-2-yl)ethane-1-sulfonamide (10)

3-Phthalimidopropanesulfonylchloride **9** (5.0 g, 18.27 mmol) was added to the mixture of aq. NH_4OH (1.16 mL/mmol) and 1,4-dioxane (1.16 mL/mmol) at 0°C, over 20 min. The reaction mixture was stirred at 0°C for 30 min and warmed to room temperature, stirred for next 3.5 h. The mixture was evaporated in vacuo to provide solid. The solid was filtered and washed

minimum amount of water to afford the title compound as off-white solid (2.55 g, 54%). R_f = 0.39 (10% MeOH in DCM). Mp = 203−205 °C. ^{1}H NMR (500 MHz, DMSO-d_6) δ_H = 7.89-7.86 (m, 2H); 7.86-7.83 (m, 2H); 7.01 (s, 2H); 3.97 (t, J = 7.55 Hz, 2H); 3.34 (t, J = 7.4 Hz, 2H); ^{13}C NMR (125 MHz, DMSO-d_6) δ_C = 167.4, 134.4 (2 carbons), 131.7, 123.0 (2 carbons), 51.6, 32.6; LRMS (ESI$^+$): m/z = 277 $[M+Na]^+$.

2-Aminoethane-1-sulfonamide hydrochloride (11)

To a phthalimido-β-aminoethanesulfonamide **10** (1.0 g, 3.93 mmol, 1.0 equiv) suspended in abs. EtOH was added 50-60% solution of hydrazine hydrate (0.48 mL, 9.83 mmol, 2.5 equiv) and the reaction mixture was refluxed for 3 h. After 3 hours, white solid was precipitated, the reaction mixture was allowed to cool at room temperature and conc. HCl (10 mL, 2.5 mL/mmol) was added. The mixture was stirred at room temperature for next 20 min, filtered through celite bed, and washed with EtOH. The filtrate was evaporated in vacuo to provide the residue, which was triturated by 2:1 EtOH-H_2O (10-15 mL) and filtered through celite bed. The filtrate evaporated in vacuo, to provide oil. Trituration of the residue, filtration through celite and evaporation in vacuo were continued for 2-3 times to provide the title compound (0.32 g, 51%) as colorless hygroscopic solid. ^{1}H NMR (500 MHz, DMSO-d_6) δ_H = 8.56 (bs, 2H); 7.23 (s, 2H); 3.43-3.40 (m, 2H, partially overlapped by water peak); 3.13-3.10 (m, 2H); ^{13}C NMR (125 MHz, DMSO-d_6) δ_C = 51.6, 34.2; LRMS (ESI$^+$): m/z = 163 $[M+K]^+$.

Protein expression and purification. hCA II protein was expressed and purified as previously described.[25] The protein sequences for human CA IX and CA XII were aligned to the human CA II sequence using Clustal-Omega. Clones of the CA IX and CA XII mimic proteins containing the CA II sequence modified by either 10 or 9 changes (respectively) in the active

site were ordered from Genescript and subsequently subcloned into pET43 using the BamH1 and Xho1 sites.

Competent BL21:DE3 cells were transformed with the respective plasmids and fresh cultures were grown at the 1 L scale in Teriffic Broth with ampicillin at 100 μg/mL with zinc added to a final concentration of 50 μM. The cells were grown at 37° C until mid-log phase (OD_{600} 0.6 to 0.8) and protein expression was induced using 0.5 mM IPTG. The cells were allowed to grow for another 4.5 hours, then centrifuged and the pellets were stored in a freezer at -20° C. The cell pellets were brought up in Tris buffered saline (TBS: 40 mM Tris at pH 8.0, 150 mM NaCl) with added 150 mM NaCl, 10 mM imidazole, 2 mM $MgCl_2$, Benzonase, complete EDTA free tablets, lysozyme, 1 mM PMSF and the cells were disrupted with three passes using a cell crusher (Avestin). The resulting slurry was centrifuged to remove cell debris and the supernatant was loaded onto a His-Trap 1mL FF column in buffer A (TBS plus 150mM NaCl, 10 mM imidazole). The column was washed with 20 column volumes (CV) of buffer A, then 20 CV of Buffer A containing 20 mM final imidazole concentration, subsequently the protein was eluted with 5 CV of buffer A containing 250 mM imidazole. The peak fractions were pooled and put onto a S200 16/60 gel filtration column in TBS and the peak fraction of monomeric protein was subsequently pooled and concentrated to 11 mg/mL for the CA-IX mimic and 10.5 mg/mL for the CA-XII mimic.

Protein X-ray Crystallography. Concentrated hCA-II at about 10 mg/mL was set up in SD-2 plates (Molecular Dimensions) with the following ratio of protein plus reservoir plus seeds: 250 nL + 225 nL + 25 nL. The plate was incubated at 20º C and the reservoir condition consisted of 2.9 M ammonium sulfate with 0.1 M Tris buffer at pH 8.3. Dry compound was added to the crystallization drop after crystals had formed and several days before data were

collected. The CA-IX mimic and CA-XII mimic proteins were crystallized in sitting drop plates using 200 nL protein at 5 mg/mL plus 200 nL reservoir solution over 50 μL reservoirs for the CA-XII mimic and 150 nL protein at 5.5 mg/mL plus 120 nL reservoir plus 30 nL micro-crystalline seeds over 50 μL reservoirs for the CA-IX mimic. The crystallization plates were incubated at two temperatures (20º C and 8º C) and large plate-like crystals were found at both temperatures in optimized ammonium sulfate conditions (2.6 to 2.8 M ammonium sulfate, 100 mM Tris pH 8.0 to 9.0). Crystals were harvested using nylon loops with the addition of glycerol as a cryoprotectant (20% final concentration). Data were collected at the Australian Synchrotron MX1 beamline in 360 one degree oscillations. The data were indexed using XDS[26] and scaled using Aimless[27]. Molecular replacement was done using Phaser[28] using 4cq0 as the initial starting model for CA II, and the human CA-II (PDB code 4NR4) as a starting model for the CA IX-mimic and CA XII-mimic, the mutated residues were built into the structures using Coot[29] . All models were manually rebuilt using Coot[29] and refined using Refmac[30]. The initial placement of **1** and the dictionary (cif) file were generated with AFITT (OpenEye Scientific Software) and further refined using Refmac.[30] The structure and structure factors were deposited in the PDB with accession code 5a6h (CA II with psammaplin C), 5g01 (CA XII mimic with psammaplin C), 5g03 (CA IX mimic with psammaplin C), 5g0b (CA IX apo) and 5g0c (CA XII apo).

CA Inhibition Assay. An applied Photophysics stopped-flow instrument was used for assaying the CA-catalyzed CO_2 hydration activity.[31] IC_{50} values were obtained from dose-response curves working at seven different concentrations of the test compound, by fitting the curves using PRISM (www.graphpad.com) and nonlinear least-squares methods; values represent the mean of at least three different determinations as described by us previously.[32] The inhibition constants (K_i) were then derived by using the Cheng-Prusoff equation as follows: $K_i = IC_{50}/(1$

+ [*S*]/K_m), where [*S*] represents the CO_2 concentration at which the measurement was carried out, and K_m is the concentration of substrate at which the enzyme activity is at half-maximal. All enzymes used were recombinant, produced in *Escherichia coli* as reported earlier.[33, 34] The hCA isoform concentrations in the assay system ranged between 7.5 and 15.0 nM.

CA activity assay. The enzymatic activity of CA II, CA IX mimic, and CA XII mimic was determined using protonography.[21] CA protein (0.5 μg each, 1 μL) and control proteins BSA and OVA (5 μg each, 2 μL each) were prepared in 1× PBS (15 uL). The samples were diluted with 5× SDS (-) buffer (5 μL) to give a final sample volume of 25 μL, and separated with SDS-PAGE (12%) at 180 V until the dye front has ran off the gel. After separation, the gel was incubated in 2.5% Triton X-100 for 1 h with shaking, followed by two times 10 min wash with 10% isopropanol (in 100 mM Tris, pH 8.2). The gel was then stained with 0.1% bromothymol blue (in 100 mM Tris, pH 8.2) for 30 min. The stained gel was then incubated in carbonated water and color change (from blue to yellow) or color retention (remained blue) was determined, within 30 s of exposing the gel to carbonated water.

Supporting Information. ^{1}H and ^{13}C NMR spectra for compounds **1**, **3-6** and **8-11**. COSY and HMBC spectra for compound **1**. HPLC chromatograms for compound **1** and **6**. Crystallography statistics and electron density images, spectral data-images of all compounds are provided. This material is available free of charge via the Internet at http://pubs.acs.org.

PDB ID Codes. All of the coordinates and structure factors have been deposited in the PDB and are available with the following codes 5a6h, 5g01, 5g03, 5g0c, 5g0b.

Corresponding author

S.-A.P. Telephone: +61 7 3735 7825; e-mail: s.poulsen@griffith.edu.au.

Keywords sulfonamide, natural product, carbonic anhydrase XII, protein mimic

Acknowledgement. We thank the Australian Research Council (grant numbers DP110100071, FT10100185 to S.-A.P.), two EU grants of the 7th framework program and Griffith University (Ph.D. scholarship to P.M. and K.T.). We thank Professor Emeritus Ian D. Jenkins for helpful discussions. We thank Dr. Tanja Grkovic for NMR discussions. We thank Dr. Lucy Woods and Dr. Wendy Loa for HRMS measurements and Anna Raicevic for expression and purification of the CA IX and CA XII mimics. We thank the CSIRO C3 Crystallisation Centre for all CA crystals, the Australian Synchrotron and beamline scientists for beam time, and OpenEye Scientific Software for a license to AFITT.

Abbreviations Used.

CA, carbonic anhydrase; hCA, human carbonic anhydrase; AZA, acetazolamide; K_i, inhibition constant; NPs, natural products; DNP, dictionary of natural products.

References

1. Neri, D.; Supuran, C. T. Interfering with pH regulation in tumours as a therapeutic strategy. *Nat. Rev. Drug Discov.* **2011**, 10, 767-777.

2. Alterio, V.; Di Fiore, A.; D'Ambrosio, K.; Supuran, C. T.; De Simone, G. Multiple Binding Modes of Inhibitors to Carbonic Anhydrases: How to Design Specific Drugs Targeting 15 Different Isoforms? *Chem. Rev.* **2012**, 112, 4421-4468.

3. Davis, R. A.; Innocenti, A.; Poulsen, S.-A.; Supuran, C. T. Carbonic anhydrase inhibitors. Identification of selective inhibitors of the human mitochondrial isozymes VA and VB over the cytosolic isozymes I and II from a natural product-based phenolic library. *Bioorg. Med. Chem.* **2010**, 18, 14-18.

4. Davis, R. A.; Hofmann, A.; Osman, A.; Hall, R. A.; Mühlschlegel, F. A.; Vullo, D.; Innocenti, A.; Supuran, C. T.; Poulsen, S.-A. Natural Product-Based Phenols as Novel Probes for Mycobacterial and Fungal Carbonic Anhydrases. *J. Med. Chem.* **2011**, 54, 1682-1692.

5. *Dictionary of Natural Products* **(DVD) version 21.1, 2012**.

6. Mujumdar, P.; Poulsen, S.-A. Natural Product Primary Sulfonamides and Primary Sulfamates. *J. Nat. Prod.* **2015**, 78, 1470-1477.

7. Jiménez, C.; Crews, P. Novel marine sponge derived amino acids 13. Additional psammaplin derivatives from Psammaplysilla purpurea. *Tetrahedron* **1991**, 47, 2097-2102.

8. Piña, I. C.; Gautschi, J. T.; Wang, G.-Y.-S.; Sanders, M. L.; Schmitz, F. J.; France, D.; Cornell-Kennon, S.; Sambucetti, L. C.; Remiszewski, S. W.; Perez, L. B.; Bair, K. W.; Crews, P. Psammaplins from the Sponge Pseudoceratina purpurea: Inhibition of Both Histone Deacetylase and DNA Methyltransferase. *J. Org. Chem.* **2003**, 68, 3866-3873.

9. Abend, A.; Kehat, I. Histone deacetylases as therapeutic targets — From cancer to cardiac disease. *Pharmacol.Ther.* **2015**, 147, 55-62.

10. Kottakota, S. K.; Benton, M.; Evangelopoulos, D.; Guzman, J. D.; Bhakta, S.; McHugh, T. D.; Gray, M.; Groundwater, P. W.; Marrs, E. C. L.; Perry, J. D.; Harburn, J. J. Versatile Routes to Marine Sponge Metabolites through Benzylidene Rhodanines. *Org. Lett.* **2012**, 14, 6310-6313.

11. Baud, M. G. J.; Leiser, T.; Meyer-Almes, F.-J.; Fuchter, M. J. New synthetic strategies towards psammaplin A, access to natural product analogues for biological evaluation. *Org. Biomol. Chem.* **2011**, 9, 659-662.

12. Nicolaou, K. C.; Hughes, R.; Pfefferkorn, J. A.; Barluenga, S.; Roecker, A. J. Combinatorial Synthesis through Disulfide Exchange: Discovery of Potent Psammaplin A Type Antibacterial Agents Active against Methicillin-Resistant Staphylococcus aureus (MRSA). *Chem. Eur. J.* **2001**, 7, 4280-4295.

13. Yoshida, M.; Saito, K.; Fujino, Y.; Doi, T. A concise total synthesis of biologically active frutinones via tributylphosphine-catalyzed tandem acyl transfer-cyclization. *Tetrahedron* **2014**, 70, 3452-3458.

14. Smits, R. A.; Adami, M.; Istyastono, E. P.; Zuiderveld, O. P.; van Dam, C. M. E.; de Kanter, F. J. J.; Jongejan, A.; Coruzzi, G.; Leurs, R.; de Esch, I. J. P. Synthesis and QSAR of Quinazoline Sulfonamides As Highly Potent Human Histamine H4 Receptor Inverse Agonists. *J. Med. Chem.* **2010**, 53, 2390-2400.

15. Hara, T.; Durell, S. R.; Myers, M. C.; Appella, D. H. Probing the Structural Requirements of Peptoids That Inhibit HDM2−p53 Interactions. *J. Am. Chem. Soc.* **2006**, 128, 1995-2004.

16. Arabshahi, L.; Schmitz, F. J. Brominated tyrosine metabolites from an unidentified sponge. *J. Org. Chem.* **1987**, 52, 3584-3586.

17. Silverstein, R. M.; Bassler, G. C.; Morrill, T. C. Spectroscopic Identification of Organic Compounds. In Wiley: New York, 1981; p 269.

18. Kopecka, J.; Campia, I.; Jacobs, A.; Frei, A. P.; Ghigo, D.; Wollscheid, B.; Riganti, C. Carbonic anhydrase XII is a new therapeutic target to overcome chemoresistance in cancer cells. *Oncotarget* **2015**, 6, 6776-6793.

19. Simpson, M.; Poulsen, S.-A. An Overview of Australia's Compound Management Facility: The Queensland Compound Library. *ACS Chem. Biol.* **2014**, 9, 28-33.

20. Pinard, M. A.; Boone, C. D.; Rife, B. D.; Supuran, C. T.; McKenna, R. Structural study of interaction between brinzolamide and dorzolamide inhibition of human carbonic anhydrases. *Bioorg. Med. Chem.* **2013**, 21, 7210-7215.

21. De Luca, V.; Del Prete, S.; Supuran, C. T.; Capasso, C. Protonography, a new technique for the analysis of carbonic anhydrase activity. *J. Enzyme Inhib. Med. Chem.* **2015**, 30, 277-82.

22. Del Prete, S.; De Luca, V.; Iandolo, E.; Supuran, C. T.; Capasso, C. Protonography, a powerful tool for analyzing the activity and the oligomeric state of the γ-carbonic anhydrase identified in the genome of Porphyromonas gingivalis. *Bioorg. Med. Chem.* **2015**, 23, 3747-3750.

23. Del Prete, S.; De Luca, V.; Supuran, C. T.; Capasso, C. Protonography, a technique applicable for the analysis of η-carbonic anhydrase activity. *J. Enzyme Inhib. Med. Chem.* **2015**, 30, 920-924.

24. Dudutiene, V.; Zubriene, A.; Smirnov, A.; Gylyt, J.; Timm, D.; Manakova, E.; Grazulis, S.; Matulis, D.; Smirnov, A. 4-Substituted-2,3,5,6-tetrafluorobenzenesulfonamides as inhibitors of carbonic anhydrases I, II, VII, XII, and XIII. *Bioorg. Med. Chem.* **2013**, 21, 2093–2106.

25. Moeker, J.; Mahon, B. P.; Bornaghi, L. F.; Vullo, D.; Supuran, C. T.; McKenna, R.; Poulsen, S.-A. Structural Insights into Carbonic Anhydrase IX Isoform Specificity of Carbohydrate-Based Sulfamates. *J. Med. Chem.* **2014**, 57, 8635-8645.

26. Kabsch, W. XDS. *Acta Crystallogr., Sect D: Biol. Crystallogr.* **2010**, 66, 125-132.

27. Evans, P. R. An introduction to data reduction: space-group determination, scaling and intensity statistics. *Acta Crystallogr., Sect D: Biol. Crystallogr.* **2011**, 67, 282-292.

28. McCoy, A. J.; Grosse-Kunstleve, R. W.; Adams, P. D.; Winn, M. D.; Storoni, L. C.; Read, R. J. Phaser crystallographic software. *J. Appl. Crystallogr.* **2007**, 40, 658-674.

29. Emsley, P.; Lohkamp, B.; Scott, W. G.; Cowtan, K. Features and development of Coot. *Acta Crystallogr., Sect D: Biol. Crystallogr.* **2010**, 66, 486-501.

30. Murshudov, G. N.; Skubák, P.; Lebedev, A. A.; Pannu, N. S.; Steiner, R. A.; Nicholls, R. A.; Winn, M. D.; Long, F.; Vagin, A. A. REFMAC5 for the refinement of macromolecular crystal structures. *Acta Crystallogr., Sect D: Biol. Crystallogr.* **2011**, 67, 355-367.

31. Khalifah, R. G. The carbon dioxide hydration activity of carbonic anhydrase. *J. Biol. Chem.* **1971**, 246, 2561-2573.

32. Lopez, M.; Drillaud, N.; Bornaghi, L. F.; Poulsen, S.-A. Synthesis of S-Glycosyl Primary Sulfonamides. *J. Org. Chem.* **2009**, 74, 2811-2816.

33. Winum, J.-Y.; Vullo, D.; Casini, A.; Montero, J.-L.; Scozzafava, A.; Supuran, C. T. Carbonic Anhydrase Inhibitors. Inhibition of Cytosolic Isozymes I and II and Transmembrane, Tumor-Associated Isozyme IX with Sulfamates Including EMATE Also Acting as Steroid Sulfatase Inhibitors. *J. Med. Chem.* **2003**, 46, 2197-2204.

34. Vullo, D.; Innocenti, A.; Nishimori, I.; Pastorek, J. r.; Scozzafava, A.; Pastoreková, S.; Supuran, C. T. Carbonic anhydrase inhibitors. Inhibition of the transmembrane isozyme XII with sulfonamides—a new target for the design of antitumor and antiglaucoma drugs? *Bioorg. Med. Chem. Lett.* **2005**, 15, 963-969.